Behavioral modeling of power amplifier for radar applications

François-Xavier Estagerie[1], Abderrazak Bennadji[1], Tibault Reveyrand[1], Sébastien Mons[1], Raymond Quéré[1] and Laurent Constancias[2]

Abstract – In the design process of modern communication systems, it is more and more required to predict accurately the performances of power amplifier (PA) on the Tx-Rx chains. This paper presents two behavioral modeling approaches for PAs used in Radar applications. The proposed approaches are based on nonlinear Scattering functions which allow to take into account strong output loading impedance mismatches, with a maximum VSWR (Voltage Standing Wave Ratio) of two. This formalism was expanded according to two fields depending on whether formalism is applied to circuit or transistor level. First application presented is a black-box modeling which allows to predict circuit performances on system level with a time cost comparable to a memoryless approach. This model has been implemented in a system simulation environment (Scilab/Scicos), thanks to a toolbox dedicated to solving implicit problems. Second application, is a gray-box modeling, called topologic approach, where the topology of the design is needed. This approach differentiates the passive and active parts of PA and so that to allow an aided design of sub-circuits since this model establishes a bilateral communication between circuit and system level. Both approaches have been validated on PA in the case of loading impedance mismatch.
Index Terms – Behavioral modeling, Impedance mismatch, Nonlinear scattering functions, System environment.

I. Introduction

In recent years the development of active electronically scanned array (AESA) radar has been significant. This technology will equip most of next generation military radar systems [1]. In the framework of the development of such systems, an accurate "system" simulation is needed. Indeed, nowadays, cost reduction of such systems is a key issue for the European defence industry (an AESA is two times more expensive than a passive electronically scanned array) and that implies the use of accurate simulation tools to decrease margins taken on component specifications. Such simulations must be able to optimize the design of the whole radar functional chain by enabling design engineers able to predict and analyse the impact of microwave components on "system" performance.
For design constraints of AESA, PA is clearly identified as a critical component since it directly impacts the gain and phase controls of each radiating element. Many disturbances are observed, such as high frequency (HF) and low frequency (LF) memory effects, thermal effects and load mismatches since design constraints of ASEA lead to significant load mismatches (up to VSWR $= 2$) with varying phase. Moreover, statistics of the process have to be impacted on T/R module performances and then on the overall Radar performances for estimating acceptable tolerances on its constitutive elements.
Several behavioral models (i.e. black-box models) have been proposed in the past years [2] and are able to predict memory effects [3, 4] or thermal effects [5, 6]. However, these models are unilateral and thus only dedicated to classical Data Flow simulators. More recently, efficient bilateral models were developed [7-9], derived from Scattering parameters formalism. But these models imply also that system simulators are able to solve implicit equations. Significant efforts have to be performed on the development of accurate system simulation tools (i.e. able to solve implicit equations) and efficient macro-models which combine accuracy, stability and fastness, in order to analyse each constitutive element and to decrease margins taken on components specifications.
This article is structured as follow; in Section II, we introduce respectively the mathematical formalism of nonlinear Scattering parameters, the extraction process, based on harmonic balance (HB) simulations or CW measurements and some results in the case of strong load mismatches. In Section III, we describe the extended formalism in order to take into account PA's operating bandwidth and then its application to the development of a black-box behavioral model for estimating during the design process the impact of load mismatch on system performances. We describe the implementation of this model in an advanced system environment (Scilab/Scicos - Modelica) which is able to compute at the same time unilateral or bilateral models. In Section IV, we describe a new behavioral approach, named topologic model, dedicated to aided design of sub-circuits since this model establishes a bilateral communication between circuit and system level. This new approach, first implemented in circuit environment, Agilent Advanced Design System (ADS) is promising for designing sub-circuits (e.g. biasing or matching circuits) and to extend model capabilities to nonlinear memories and thermal effects. Various results are given to illustrate the predictive capabilities of these approaches on S-band and X-band PAs used for Radar applications.

II. Nonlinear Scattering functions

A) Model theory

The Scattering parameters formalism, applied to weakly non linear devices, was introduced in the first time in [10]

Received September 30th, 2007. Revised December 21th, 2007.
[1]XLIM, UMR CNRS n 6172 - University of Limoges, 123 Avenue Albert Thomas, 87060 Limoges Cedex, France;
E-mail: fx.estagerie@gmail.com; [2]ONERA, Chemin de la Hunière, FR-91761, Palaiseau Cedex, France.

and dedicated to amplifier's modeling in [11]. These works are based on a extension of Scattering parameters by using Volterra series. However, the accuracy of this formalism is relative to the number of Volterra kernels used and so can lead to a complex extraction processing. Though effective in low level signal excitation, this PA's model isn't efficient in nonlinear operating.

More recently, robust model has been established thanks to nonlinear Scattering functions, introduced by [7] and developed in [8]. In our article, PA is described thanks to a reduction of nonlinear Scattering functions. Indeed, we are making the assumption that an amplifier can be viewed as a nonlinear two-port circuit at the fundamental frequency without memory effects. It is defined by the following relationship:

$$\tilde{b}_i = f_{NLi}\left(\tilde{a}_1, \tilde{a}_1^*, \tilde{a}_2, \tilde{a}_2^*\right) \tag{1}$$

where $i = 1, 2$. $\tilde{b}_1$, $\tilde{b}_2$ and $\tilde{a}_1$, $\tilde{a}_2$ are respectively the reflected and incident power waves at the two ports. Considering the condition of weak to moderate loading impedance mismatch (i.e. it means $\tilde{a}_2 \prec\prec \tilde{a}_1$), expansion of $\tilde{b}_i$ into first order Mc Laurin series gives equation (2):

$$\begin{aligned}\begin{pmatrix}\tilde{b}_1\\ \tilde{b}_2\end{pmatrix} &= \begin{pmatrix}S_{11}(|\tilde{a}_1|) & S_{12}(|\tilde{a}_1|)\\ S_{21}(|\tilde{a}_1|) & S_{22}(|\tilde{a}_1|)\end{pmatrix}\cdot\begin{pmatrix}\tilde{a}_1\\ \tilde{a}_2\end{pmatrix}\\ &+\begin{pmatrix}0 & S_{12}^{\Delta}(|\tilde{a}_1|)\\ 0 & S_{22}^{\Delta}(|\tilde{a}_1|)\end{pmatrix}\cdot\begin{pmatrix}\tilde{a}_1^*\\ \tilde{a}_2^*\end{pmatrix}\end{aligned} \tag{2}$$

Where $S_{ij}(|\tilde{a}_1|)$ are the nonlinear Scattering functions that depend only on the incident wave's magnitude. Thus, equation (2) ensures the validity of the bilateral model of nonlinear part at operating frequency.

B) Extraction procedure

The identification of nonlinear Scattering functions, in equation (2), is obvious and requires only HB simulations or CW measurements at the PA's operating frequency. As shown in Fig. 1(a), input/output currents and voltages are extracted from three different loading impedances, located on Smith chart in Fig. 1(b):

- $Z_1 = 50\ \Omega\ (\Gamma_1 = 0)$
- $Z_2 = 75\ \Omega\ (\Gamma_2 = 0.2\cdot\exp(j\cdot 0))$
- $Z_3 = (46.2 + j\cdot 19.2)\ \Omega\ (\Gamma_3 = 0.2\cdot\exp(j\cdot\pi/2))$

where Γ is the reflected coefficient associated to the PA's load. This approach can be derived either from commonly available circuit simulation tools (HB) of from common physical measurements equipments (Vectorial Network Analyser load-pull setup [12]). The currents and voltages are then converted into incident and reflect waves. Three load impedances are sufficient to solve the 3x3 linear sys-

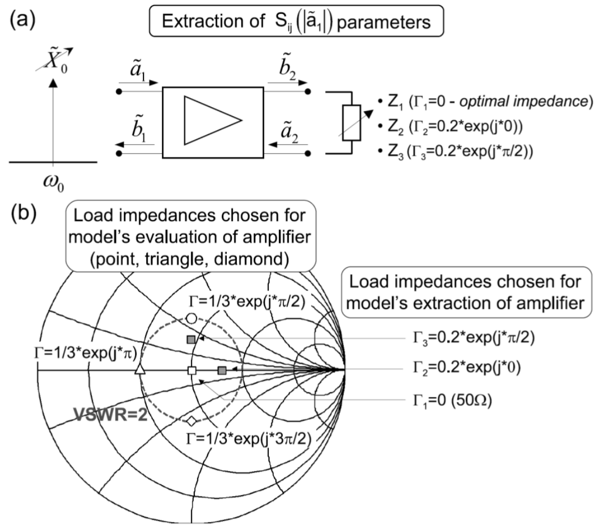

Fig. 1. Nonlinear Scattering functions extraction setup. Load impedances chosen to extract and validate the model.

tem of equation (3) for different input powers:

$$\begin{pmatrix}S_{11}\\ S_{12}\\ S_{12}^{\Delta}\\ S_{21}\\ S_{22}\\ S_{22}^{\Delta}\end{pmatrix} = \begin{pmatrix}\tilde{a}_{1_1} & \tilde{a}_{2_1} & \tilde{a}_{2_1}^* & 0 & 0 & 0\\ 0 & 0 & 0 & \tilde{a}_{1_1} & \tilde{a}_{2_1} & \tilde{a}_{2_1}^*\\ \tilde{a}_{1_2} & \tilde{a}_{2_2} & \tilde{a}_{2_2}^* & 0 & 0 & 0\\ 0 & 0 & 0 & \tilde{a}_{1_2} & \tilde{a}_{2_2} & \tilde{a}_{2_2}^*\\ \tilde{a}_{1_3} & \tilde{a}_{2_3} & \tilde{a}_{2_3}^* & 0 & 0 & 0\\ 0 & 0 & 0 & \tilde{a}_{1_3} & \tilde{a}_{2_3} & \tilde{a}_{2_3}^*\end{pmatrix}^{-1} \cdot \begin{pmatrix}\tilde{b}_{1_1}\\ \tilde{b}_{2_1}\\ \tilde{b}_{1_2}\\ \tilde{b}_{2_2}\\ \tilde{b}_{1_3}\\ \tilde{b}_{2_3}\end{pmatrix} \tag{3}$$

where $\tilde{a}_{i_j}$ is the incident wave at the port i when PA terminated with Z_j (Fig. 1).

C) Simulation results

The proposed behavioral modeling was applied to an S-Band PA (2.1 GHz), based on InGaP/GaAs HBTs. The small gain is 11.6 dB and the power characteristics are respectively an output power of 42.7 dBm (18.6 W) at 1 dB gain compression with an associated power-added efficiency (PAE) of 63.8 %.

Extraction and validation of the model have been realized in ADS, through HB simulations, at PA's operating frequency. The model has been implemented thanks to an FDD (Frequency-domain Defined Device) nonlinear block, likewise in [9], where the equation (2) defines the relationships between the input/output ports.

Fig. 2 shows the PA's nonlinear Scattering functions extracted, in dB and phase. It appears that S_{ij}^{Δ} (dashed lines on Fig. 2) haven't any influence in low level excitation. Close to PA's nonlinear operating, S_{ij}^{Δ} levels are comparable with the others Scattering functions levels, in particular S_{22}^{Δ}.

The dashed circle on Smith chart in Fig. 1(b) is associated to a VSWR of two for all the phases. The circle, triangle, and diamond plotted on the dotted lines mean load impedances chosen for evaluating the PA performances under mismatch conditions. The white square symbolizes

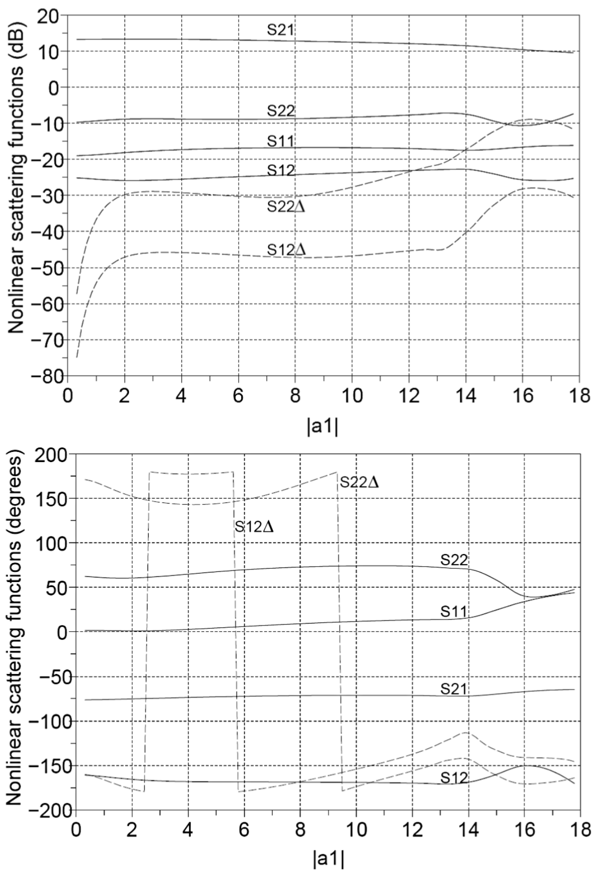

Fig. 2. PA's nonlinear scattering functions (dB) and (phase) versus $\tilde{a}_1$.

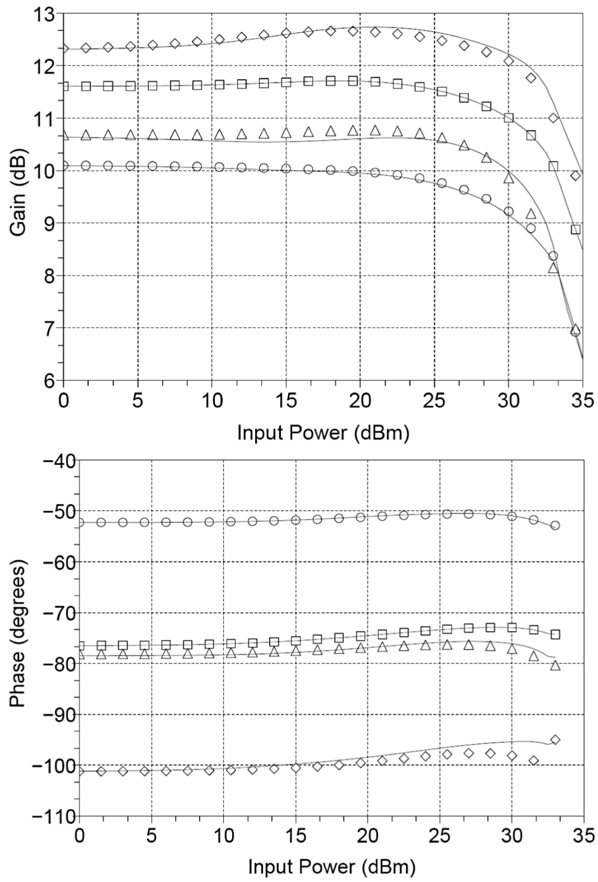

Fig. 3. Simulation-based behavior model (solid lines) compared to circuit. Gain (dB) and AM-PM (degrees) versus input power in dBm for PA terminated with the different loads symbolized on Fig. 1(b).

the optimal load equal to 50 Ω. Fig. 3 shows the comparison between circuit-level simulation and our model at operating frequency, when the PA is respectively connected to its optimal load and to the three different loads (VSWR = 2).

We notice that, when the output impedance is equal to one of the load used to PA's identification (like 50 Ω), circuit and model responses are identical, because of the system (3) is solved from incident/reflect waves measured at these impedances.

For other loads which belong to the disc of VSWR = 2, errors are almost null. In the worst conditions, ($\Gamma = 1/3 \cdot \exp(j \cdot 3\pi/2)$) the upper gain deviation between model and circuit simulation is close to 0.3 dB at −4 dB compression. These results demonstrated the model abilities for predicting PA's behavior until a VSWR of two.

III. Black-box modeling for accurate predictions of PA's performances

A) From operating frequency to amplifier's bandwidth

The model's capabilities are extended to PA's operating bandwidth, in order to take into account the PA's HF memory effects [8, 13, 14], which are significant in Radar applications. The nonlinear Scattering functions extraction is recurred for several frequencies which belong to PA's bandwidth. Equation (4) defines the PA's model:

$$\begin{pmatrix}\tilde{b}_1\\ \tilde{b}_2\end{pmatrix} = \begin{pmatrix} S_{11}(|\tilde{a}_1|,\Omega) & S_{12}(|\tilde{a}_1|,\Omega)\\ S_{21}(|\tilde{a}_1|,\Omega) & S_{22}(|\tilde{a}_1|,\Omega)\end{pmatrix}\cdot\begin{pmatrix}\tilde{a}_1\\ \tilde{a}_2\end{pmatrix} + \begin{pmatrix}0 & S_{12}^{\Delta}(|\tilde{a}_1|,\Omega)\\ 0 & S_{22}^{\Delta}(|\tilde{a}_1|,\Omega)\end{pmatrix}\cdot\begin{pmatrix}\tilde{a}_1^*\\ \tilde{a}_2^*\end{pmatrix} \tag{4}$$

where Ω is the frequency offset from carrier.

B) Advanced system environment: Scilab/Scicos - Modelica

The system simulation environment chosen, Scilab/Scicos, is an open-source alternative to Matlab/Simulink. Scicos is a toolbox in the free scientific software package for numerical computations available in Scilab [15]. It is dedicated to the modeling and simulation of dynamic systems. Several RF simulation tools were implemented in Scicos, like numerical transmission chains [16], accurate unilateral black-box models [17] and a co-simulation interface between circuit and system simulator. The choice of the system simulator Scicos was driven by the capability to couple Scicos and Modelica, which is a freely available object-oriented language [18, 19]. Modelica is used for solving physical problems, based on DAE system (Differential Algebraic Equation) [20]. Indeed, bilateral modeling implies that a simulation environment can solve implicit systems, i.e. DAE system in the following form:

$$F\left(\dot{x}, x, \dot{y}, y, t\right) = 0 \tag{5}$$

Considering the second equation given in (4), we can rewrite the real and imaginary parts of the output wave $\tilde{b}_2$ (where $\tilde{a}_i$ and $\tilde{b}_i$ are time dependent) :

$$\left\{ \begin{aligned} \tilde{b}_2^{\Re} = {} & S_{21}^{\Re}\left(|\tilde{a}_1|, \Omega\right) \cdot \tilde{a}_1^{\Re} - S_{21}^{\Im}\left(|\tilde{a}_1|, \Omega\right) \cdot \tilde{a}_1^{\Im} \\ & + S_{22}^{\Re}\left(|\tilde{a}_1|, \Omega\right) \cdot \tilde{a}_2^{\Re} - S_{22}^{I}\left(|\tilde{a}_1|, \Omega\right) \cdot \tilde{a}_2^{\Im} \\ & + {S_{22}^{\Delta}}^{\Re}\left(|\tilde{a}_1|, \Omega\right) \cdot \tilde{a}_2^{\Re} + {S_{22}^{\Delta}}^{\Im}\left(|\tilde{a}_1|, \Omega\right) \cdot \tilde{a}_2^{\Im} \\ \tilde{b}_2^{\Im} = {} & S_{21}^{\Im}\left(|\tilde{a}_1|, \Omega\right) \cdot \tilde{a}_1^{\Re} + S_{21}^{\Re}\left(|\tilde{a}_1|, \Omega\right) \cdot \tilde{a}_1^{I} \\ & + S_{22}^{\Im}\left(|\tilde{a}_1|, \Omega\right) \cdot \tilde{a}_2^{\Re} + S_{22}^{\Re}\left(|\tilde{a}_1|, \Omega\right) \cdot \tilde{a}_2^{\Im} \\ & + {S_{22}^{\Delta}}^{\Im}\left(|\tilde{a}_1|, \Omega\right) \cdot \tilde{a}_2^{\Re} - {S_{22}^{\Delta}}^{\Re}\left(|\tilde{a}_1|, \Omega\right) \cdot \tilde{a}_2^{\Im} \end{aligned} \right. \tag{6}$$

A more convenient form of equation (6) is obtained by considering the reflected Γ coefficient associated to the PA's load:

$$\tilde{a}_2(t) = \Gamma \cdot \tilde{b}_2(t) \tag{7}$$

In this case, equations (6) and (7) takes the following form:

$$F\left(\tilde{a}_1(t), \tilde{b}_2(t), t\right) = 0 \tag{8}$$

In order to simplify diagram construction, acausal (or implicit) blocks, i.e. blocks with non-oriented input/output ports, are integrated in Scicos. Indeed, these blocks are written obviously in Modelica language but external functions can be called. Note that, explicit and implicit blocks can be used simultaneously in the same Scicos diagram (in this case, DAE solver is chosen). The compilation of Scicos diagrams generates a Modelica netlist that describes the entire diagram in a temporary file. The Modelica compiler, called Modelicac, receives this netlist and generates a usable C program for Scicos.

Equation (4), in form of equation (6), has been implemented in Modelica where $S_{ij}\left(|\tilde{a}_1|, \Omega\right)$ are expanded thanks to polynomials approximation:

$$S_{ij}\left(|\tilde{a}_1|, \Omega\right) = \sum_{n=0}^{N} \alpha_n\left(|\tilde{a}_1|\right) \cdot (\Omega)^n \tag{9}$$

where $i, j = 1, 2$, α_n are the polynomials coefficients and Ω a frequency parameter of this model.

This interpolation method has been chosen considering the numerical implementation of the model in system simulator and on the other hand because it offers a sufficient accuracy compared to more effective but more complex interpolation methods.

In our case, 9 frequencies are sufficient to describe the full PA's operating bandwidth (400 MHz). The polynomials degrees are weak, ranging between 3 and 5; 3 and 4 for the "classical" Scattering functions (S_{11}, S_{12}, S_{21}, S_{22}) and 5 for $\left(S_{ij}^{\Delta}\right)$ whose variations are strongly nonlinear.

C) Simulation results in time domain at system level

Fig. 4 illustrates the principle, used in Scicos, in order to simulate the PA's model in the time domain. Explicit blocks (Scicos Blocks) are dedicated to signal processing: generating excitation signals and processing simulation results. Implicit blocks (Modelica blocks) are dedicated to solving the bilateral physical system.

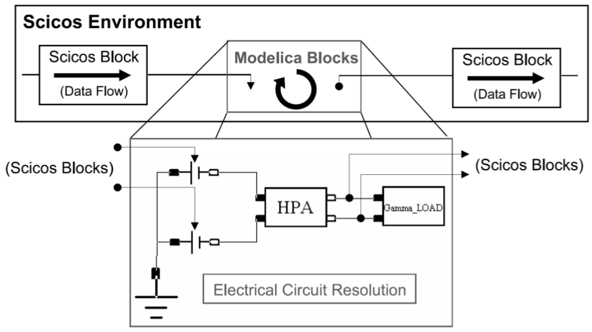

Fig. 4. Simulation of physical systems in Scicos environment.

To validate the proposed modeling implementation in system environment, it was applied to the S-Band PA.

The first comparison is made between circuit-level envelope simulation (ADS) and its system-level time domain simulation (Scicos) for the different load impedances illustrated on Smith chart Fig. 1(b). The PA is submitted to a pulse excitation at its operating frequency. The pulse magnitude is 30 dBm (1 dB compression) and 10 µs length. Fig. 5 compares the model prediction against the envelop circuit simulation of output response. The agreement is fairly good between circuit and system model.

As expected, we note that after the pulse edge, a few microseconds are necessary to obtain the pulse magnitude steady-state since this stimulus is well suited to exhibit nonlinear memory effects [21].

A second comparison is done by varying the operating frequency. Thus, in Fig. 6, the PA is submitted to a signal pulse excitation at different frequencies which belong to PA's bandwidth. PA is terminated with a load equivalent to VSWR $= 2$ ($\Gamma = 1/3 \cdot \exp\left(j \cdot 3\pi/2\right)$). The pulse magnitude is 30 dBm and 10 µs length. Fig. 6 confirms thus the good prediction of PA's behavior for any frequency in it bandwidth.

The good prediction of the PA output obtained for Radar stimuli shows the effectiveness of the proposed approach over a large bandwidth. The implementation has been shown to be suitable to system-level simulator guarantying simulation speed: the computing time of the model in Scicos is equivalent to a memoryless simulation (AM/AM - AM/PM @ f_0) in a data flow simulator, we note a time

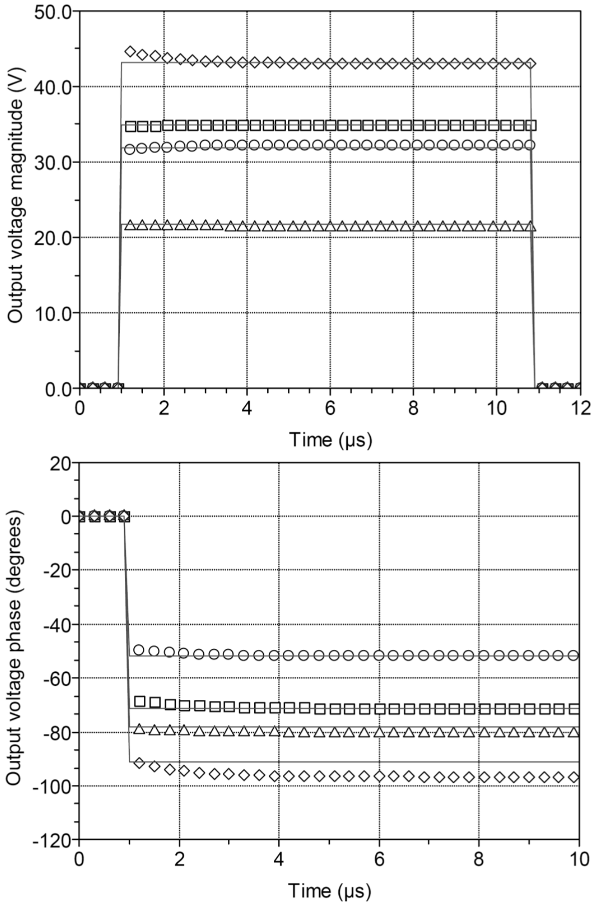

Fig. 5. Simulation-based behavior model (solid lines) compared to circuit time response. Output voltage magnitude (V) and phase (degrees) versus time in µs for PA terminated with the different loads show on Smith chart in Fig. 1(b).

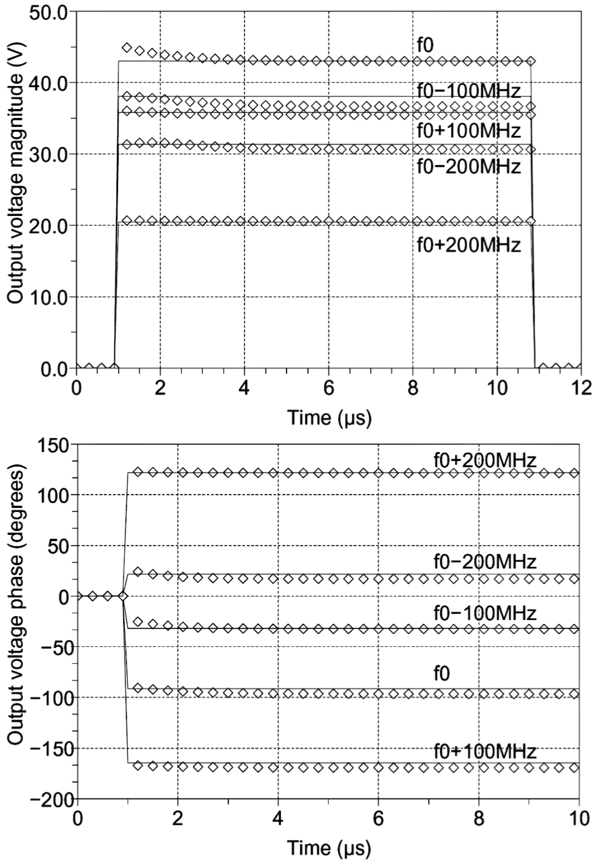

Fig. 6. Simulation-based behavior model (solid lines) compared to circuit time response. Output voltage magnitude (V) and phase (degrees) versus time in µs for PA terminated with load equivalent to VSWR = 2 ((40-j.30)Ω) at different frequencies which belong to PA's bandwidth.

gain up to 150 compares to the envelop circuit simulation level.

IV. Topologic modeling for an efficient design of PA's sub-circuit

Black-box modeling is very useful for estimating circuit performances on system level. Unfortunately, this approach cannot be used to investigate nonlinear phenomena involved in critical circuits such as multistage PAs used in the emission chain. There is an interest on identification of electrical and electro-thermal causes of memory since this phenomena are as a majority located in particular sub-circuits such as active cells, biasing or matching networks. This novel modeling approach differentiates also the passive (order reduction) and active (nonlinear Scattering functions) parts and thus allows an efficient modeling of each sub-circuit effectively. Thereby, this approach is useful to impact circuit performances at system level but also to provide an optimal designing of each sub-circuit. Hence, topologic modeling establishes a bilateral communication between circuit and system level, allowing an efficient aided design of PAs.

A) Model theory

The approach is directly derived from the topology of the amplifier. Thus, this model is divided into linear and nonlinear sub-models, respectively associated to passive and active elements [22]. In order to take into account output impedance mismatch, linear and nonlinear models are described in a bilateral way.

Passive elements, which are responsible for the most of simulation time cost and HF memory effects, are described in circuit environment thanks to their linear Scattering parameters. They will be implemented through reduce order techniques in system level simulator [23], for guarantying simulation speed.

Nonlinear Scattering functions are used to describe the transistors. The model complexity can be reduced since the impedances presented to each transistor, for a same PA's stage, are usually very close. As a result, passive cells can be viewed as two-port structures: a single nonlinear sub-model is sufficient for each stage if input/output currents are divided by the number of transistors for this stage. This model reduction enables us to use a single extraction for all transistors of a same stage and to enhance simulation time cost. Fig. 7 shows an example of the model's topology. In the following, the paper focuses on the modeling of transistors.

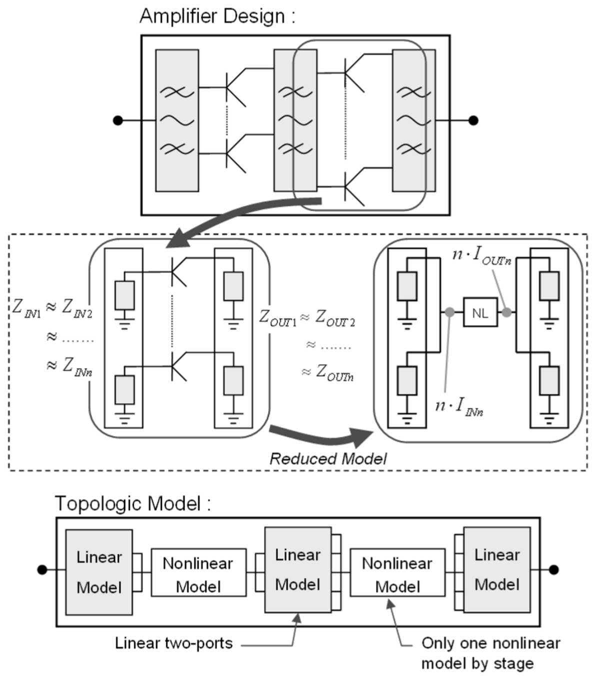

Fig. 7. Topologic approach : assembly of linear and nonlinear sub-models, based on the same topology of design circuit.

B) Nonlinear Scattering functions balanced in frequency

To extend prediction capabilities to PA's operating bandwidth, in addition to PA's HF memory effects caused by linear sub-circuits, the frequency's dispersion of transistor must be considered. An acceptable solution leads to consider $|\tilde{a}_1|$ and Ω as independent variables and thus to apply coefficient $c_{ij}(\Omega)$ (normalized to one), where $\Omega = 2\pi(f - f_0)$ is the pulsation shift with respect to reference ω_0. These coefficients are evaluated for a fixed value of $|\tilde{a}_1|$ according to a small signal regime:

$$c_{ij}(\Omega) = \left. \frac{S_{ij}(|\tilde{a}_1|, \Omega)}{S_{ij}(|\tilde{a}_1|, \Omega_0)} \right|_{|\tilde{a}_1|=\text{constant}} \tag{10}$$

Applying equations (10) into (2), we obtain:

(11)

$$\begin{pmatrix} \tilde{b}_1 \\ \tilde{b}_2 \end{pmatrix} = \begin{pmatrix} S_{11}(|\tilde{a}_1|) \cdot c_{11}(\Omega) & S_{12}(|\tilde{a}_1|) \cdot c_{12}(\Omega) \\ S_{21}(|\tilde{a}_1|) \cdot c_{21}(\Omega) & S_{22}(|\tilde{a}_1|) \cdot c_{22}(\Omega) \end{pmatrix} \cdot \begin{pmatrix} \tilde{a}_1 \\ \tilde{a}_2 \end{pmatrix} + \begin{pmatrix} 0 & S_{12}^{\Delta}(|\tilde{a}_1|) \cdot c'_{12}(\Omega) \\ 0 & S_{22}^{\Delta}(|\tilde{a}_1|) \cdot c'_{22}(\Omega) \end{pmatrix} \cdot \begin{pmatrix} \tilde{a}_1^* \\ \tilde{a}_2^* \end{pmatrix}$$

Thus, equation (11) ensures the validity of the bilateral model of nonlinear part for PA's bandwidth. $c_{ij}(\Omega)$ identification, illustrated on Fig. 8(a), is obvious by repeating the same extraction process: a constant low level excitation for each frequency offset from carrier for the three load impedances located on Smith chart on Fig. 8(b). This method implies a faster extraction process than that used for black-box modeling, as shown in Section III, without loss of accuracy.

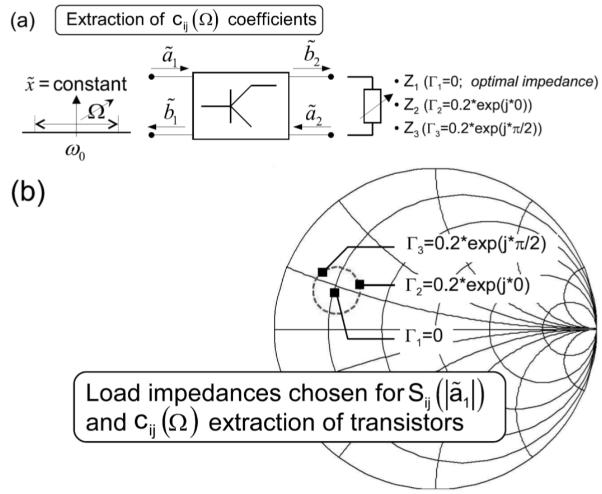

Fig. 8. Nonlinear scattering functions balanced in frequency extraction setup.

C) Implementation

Extraction and validation of the PA's model have been performed in ADS on full PA's operating bandwidth. Data files from S-Parameters passive element's simulation describe linear parts while FDD nonlinear block are standing for transistors, where the equation (11) defines the relationships between the input/output ports.

D) Simulation results in frequency domain

The proposed model was applied to a 2 stages InGaP/GaAs HBTs X-band PA, operating at $f_0 = 10.25$ GHz. Power characteristics are respectively an output power of 39 dBm (7.9 W) with an associated small gain of 17.5 dB and 34 % of PAE.

Fig. 9 gives a comparison between HB circuit simulations and HB topologic model simulations when the PA is connected with its optimal load and the three different loads (VSWR $= 2$) located on Smith chart in Fig. 9. The accuracy of topologic model results can be observed. When the load belong to the disc of VSWR $= 2$, errors are almost null. In the worst conditions, ($\Gamma = 1/3 \cdot \exp(j \cdot \pi)$) the gain deviation between model and circuit simulation is close to 0.1 dB at -1 dB compression. These results show the model's abilities to predict the PA's behavior with a good accuracy for impedance mismatch until VSWR $= 2$. Moreover some experiments were performed up to VSWR $= 3$ showing the capability of the model to take into account moderate VSWR at the price of a small degradation of performances (≤ 1 dB). The bilateral model is thus validated on full PA's bandwidth.

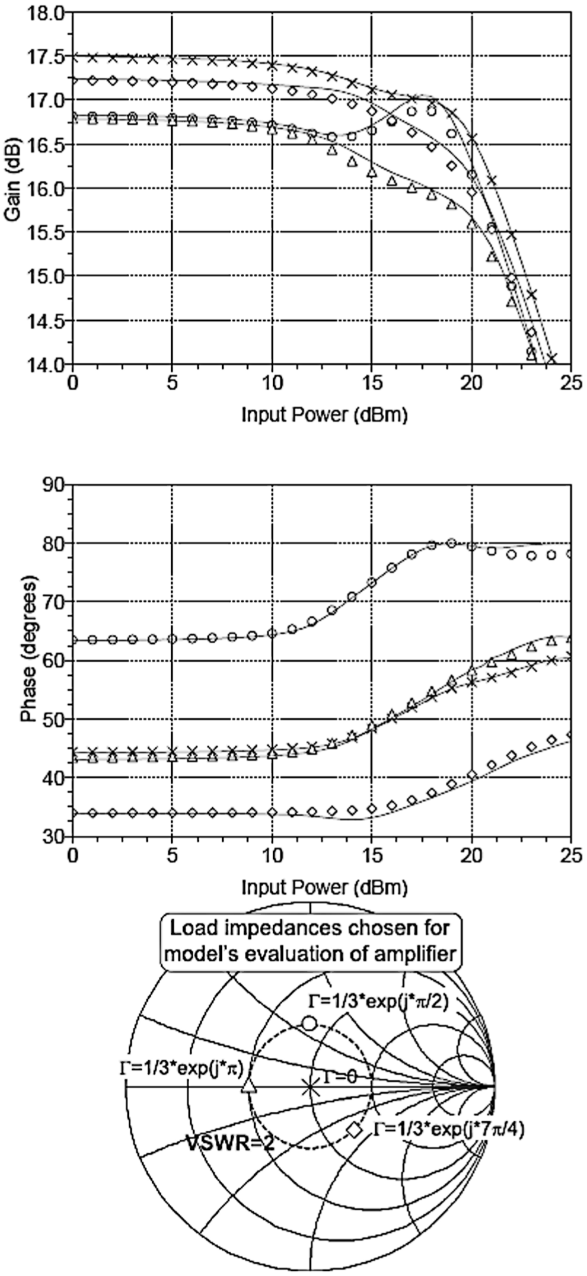

Fig. 9. Simulation-based behavior model (solid lines) compared to circuit. Gain (dB) and AM-PM (degrees) versus input power in dBm for PA terminated with the different loads shown on Smith chart.

Fig. 10 compares the performances of model against the circuit simulation in the output power-operating frequency plane. One may see a good agreement even at high power levels and out of band frequencies.
The approach is under development, next step will consider the model's implementation in system level simulator (Scilab/Scicos) where linear parts will be described thanks to poles/zeros formalism to guaranty an efficient fastness/accuracy compromise.

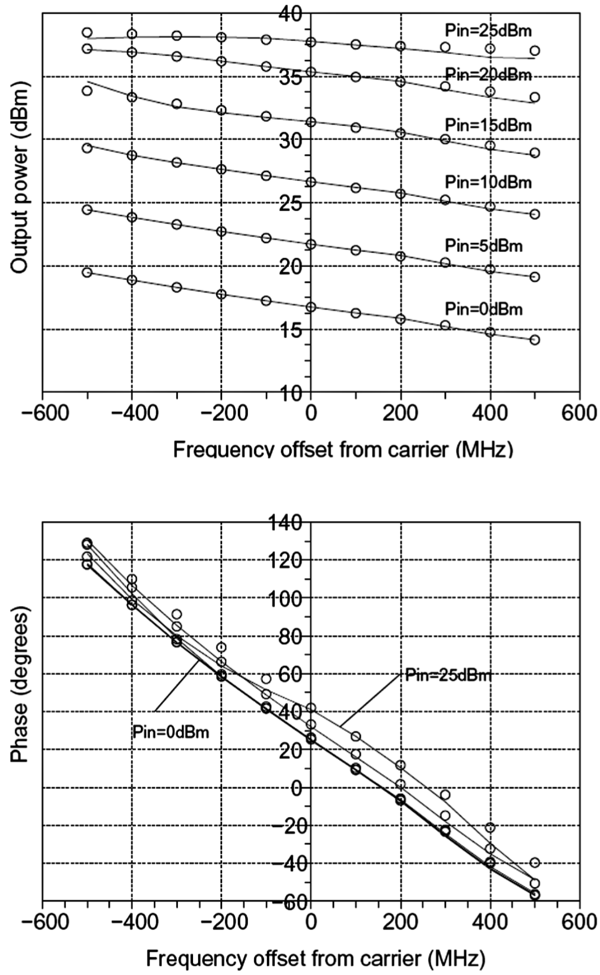

Fig. 10. Simulation-based behavior model (solid lines) compared to circuit (circles). At different input levels, output power (dBm) and output phase (degrees) versus frequency shift from carrier for PA terminated with a load equivalent to VSWR = 2 ((40-j.30) Ω).

V. Conclusion

We have presented two bilateral behavioral models dedicated to Radar applications. These models are based on nonlinear Scattering functions which allow a prediction at level system of the amplifier's behavior subjected to significant load mismatches (VSWR up to VSWR = 2).
First application is a bilateral black-box model for estimating on system level the impact of a PA submitted to a significant load mismatch. This model has been implemented in a high-level simulation tool, Scilab/Scicos - Modelica, which is able indifferently to solve both bilateral and unilateral models thanks to its ODE/DAE solvers in opposition to the common Data Flow environments. Results presented here on an S-Band power amplifier demonstrates the impact of a load mismatch on pulsed signal. This model is also well suited for predicting system performances during the design step since on one hand its extraction processing is obvious, on the other hand its computation is equivalent to a common memoryless modeling.

Second application is a bilateral topologic model which makes it possible to predict system performances but also an efficient design of sub-circuits in order to decrease margins taken on components specifications. This model, currently implemented in ADS, is under development to extend its capabilities to thermal and memory effects prediction.
These models will be very useful in establishing predictive performances in radar applications, particularly to quantify the impact of its operating on T/R modules, they should finally integrate the AESA radar simulation tools: ASTRAD and SAFAR.

Acknowledgements

The authors wish to acknowledge CELAR (Centre d'Electronique de l'ARmement) and DGA (French Defence and Security Agency) for technical and financial supports.

References

[1] Hommel, H.; Feldle, H.P.: Current status of Airborne active phased array (AESA) radar systems and future trends. European Microwave Conference, Amsterdam, Netherlands, 2004, 1517-1520.
[2] Pedro, J.C.; Maas, S.A: A comparative overview of microwave and wireless power-amplifier behavioral modeling approaches. IEEE Trans. Microwave Theory and Techniques **53** (2005), 1150-1163.
[3] Soury, A.; Ngoya, E.; Nébus, J.M.: A new behavioral model taking into account nonlinear memory effects and transient behaviors in wideband SSPAs. IEEE MTT-S Int. Microwave Symp. Digest, June 2002, 853-856.
[4] Mazière, C.; Soury, A.; Ngoya, E.; Nébus, J.M.: A system level model of solid state amplifiers with memory based on a non linear feedback loop principle. European Microwave Conference, Paris, France 2005.
[5] Boumaiza, S.; Ghannouchi, F.M.: Thermal memory effects modeling and compensation in RF power amplifiers and predistortion linearizers. IEEE Trans. Microwave Theory and Techniques **51** (2003), 2427-2433.
[6] Mazeau, J.; Sommet, R.; Caban-Chastas, D.; Gatard, E.; Quéé, R.; Mancuso, Y.: Behavioral thermal modeling for microwave power amplifier design. IEEE Trans. Microwave Theory and Techniques **55** (2007), 2290-2297.
[7] Verspecht, J.: Scattering functions for nonlinear behavioral modeling in frequency domain. Fundamentals of Nonlinear Behavioral Modeling: Foundations and Applications Workshop, IEEE MTT-S Int. Microwave Symp., June 2003.
[8] Soury, A. ; Ngoya, E.; Rousset, J.: Behavioral modeling of RF and microwave circuit blocks for hierarchical simulation of modern transceivers. IEEE MTT-S Int. Microwave Symp. Digest, June 2005, 975-978.
[9] Root, D.E.; Verspecht, J.; Sharrit, D.; Wood, J.; Cognata, A.: Broad-band poly-harmonic distortion (PHD) behavioral models from fast automated simulations and large-signal vectorial network measurements. IEEE Trans. Microwave Theory and Techniques **53** (2005), 3656-3664.
[10] Wiener, D.; Naditch, G.: A scattering variable approach to the Volterra analysis of nonlinear systems. IEEE Trans. Microwave Theory and Techniques **24** (1976), 422-433.
[11] Verbeyst, F.; Vanden Bossche, M.: VIOMAP, the S-parameter equivalent for weakly nonlinear RF and microwave devices. IEEE Trans. Microwave Theory and Techniques **42** (1994), 2531-2535.
[12] Reveyrand, T.; Gasseling, T.; Barataud, D.; Mons, S.; Nébus, J.M.: A smart load-pull method to safely reach optimal matching impedances of power transistors. IEEE MTT-S Int. Microwave Symp. Digest, June 2007, 1489-1492.
[13] Vuolevi, J.H.K; Rahkonen, T.; Manninen, J.P.A.: Measurement technique for characterizing memory effects in RF power amplifiers. IEEE Trans. Microwave Theory and Techniques **49** (2001), 1383-1389.
[14] Ngoya, E.; Le Gallou, N.; Nébus, J.M.; Burêt, H.; Reig, P.: Accurate RF and microwave system level modeling of wide band nonlinear circuits. IEEE MTT-S Int. Microwave Symp. Digest, June 2000, 79-82.
[15] Nikoukhah, R.; Steer, S.: A dynamic system builder and simulator, in User's guide - Version 1.0. [Online] Available: http://www.inria.fr/rrr/rt-0207.html.
[16] Layec, A.; Bennadji, A.; Nallatamby, J.C.; Quéré, R.; Ngoya, E.: Modeling of a communication chain components & principles of simulation in the Scilab/Scicos environment. Proc. of the 2005 IEEE Conf. on Control Applications, Toronto, Canada, August 2005, 1127-1133.
[17] Bennadji, A.; Layec, A.; Soury, A.; Mallet, A.; Ngoya, E.; Quéré, R.: Modeling of a communication chain with implementation of a Volterra power amplifier model for efficient system level simulation. The European Conference on Wireless Technology, October 2005, 101-104.
[18] Najafi, M.; Furic, S.; Nikoukhah, R.: SCICOS: a general purpose modeling and simulation environment. Proc. 4th Int. Modelica Conference, Hambourg, Germany, March 2005, 367-374.
[19] The Modelica website [Online]. Available: http://www.Modelica.org.
[20] Najafi, M.; Nikoukhah, R.; Campbell, S.L.: ODE and DAE solvers in Scicos environment. Iasted Int. Conference on applied simulation and modeling, ASM2004, Rhodes, Greece, June, 2004.
[21] Bosch, W.; Gatti, G.: Measurement and simulation of memory effects in predistortion linearizers. IEEE Trans. Microwave Theory and Techniques **37** (1989), 1885-1890.
[22] Estagerie, F.X.; Reveyrand, T.; Mons, S.; Quéré, R.; Constancias, L.; Le Helleye, P.: From circuit topology to behavioural model of power amplifer dedicated to radar applications. IEEE Electronics Letters **43** (2007), 477-479.
[23] Casas, F.J.; Portilla. J.; Quéré, R.; Mallet, A.; Villemazet, J.F.: Model-order reduction of linear and weakly nonlinear time-varying RF and microwave circuits. IEEE Trans. Microwave Theory and Techniques **52** (2004), 2262-2273.

François-Xavier Estagerie was born in France in 1981. He received the master research degree in 2004 from the Limoges University, France. He is presently a Ph.D. student at the XLIM laboratory in the High Frequency Components Circuits Signals and Systems department, Limoges University. His main interests are modeling and implementation of amplifier models in system simulator.

Abderrazak Bennadji was born in Chlef, Algeria, in 1975. He received the Electronic engineering Degree from University of Blida, Algeria, in 1999, the Phd degree in electronic from the University of Limoges. From 2006, he works in institute of microwave and optical communications, University of Limoges, where he is currently involved with modeling and implementation of the amplifier models in the system simulators.

Tibault Reveyrand was born in 1974 in Paris. He received a Ph.D. from the Limoges University, France, in 2002. From 2002 to 2004, he was postdoctoral scientist with the Centre National d'Etudes Spatiales (CNES) (French Space Agency). In 2005, he became a contractual engineer at the Centre National de la Recherche Scientifique (CNRS) with XLIM (formerly IRCOM), Limoges, France. His main research interests include the characterization and the modeling of RF and microwave non-linear components.

Sébastien Mons was born in Limoges (France) in 1970. He received the Ph.D. Degree in Electronics from the University of Limoges in 1999. He joined the Microwave Laboratory of the CNES of Toulouse, France, in 1999. Since October 2001, he is a researcher of the French CNRS at XLIM institute, Limoges university. His main research interests include system level modeling and nonlinear analysis of microwaves circuits.

Raymond Quéré (senior member IEEE) received the electrical engineering degree from ENSEEIHT Toulouse, France in 1976, the French aggregation in applied physics in 1978 and a Ph.D. degree from Limoges University in 1989. In 1992 he was appointed full professor at the Limoges University where he leads the nonlinear high frequency devices, circuits and systems research group at XLIM-CNRS laboratory. His main field of interest is in the area of nonlinear device and circuit modeling with a particular emphasis on nonlinear phenomena such as stability in power amplifiers. He is involved in a number of technical program committees and serves as a reviewer for several journals. In 2005 he was appointed as the general Chairman of the European Microwave Week in Paris.

Laurent Constancias received in 2003 the degree in electrical and computer engineering (Ecole Supérieure d'Electricité). Between 2003-2007, he was microwave engineer at CELAR (French MoD, DGA). Since 2007, he joined research and development radar engineer at ONERA, the french aerospace lab. His main interests include microwave components, propagation, signal processing applied to radar and numeric communications, modeling and numeric simulation.